Head-on versus Side-on [5−5]Bitrovacenes Featuring Benzene and Naphthalene Units as Spacers: How π-Stacking Affects Exchange Coupling and Redox Splitting†

Christoph Elschenbroich,* Matthias Wolf, Olav Schiemann, Klaus Harms, Olaf Burghaus, and Jürgen Pebler

Fachbereich Chemie der Philipps-Universität, D-35032 Marburg, Germany

Received July 2, 2002

The biradicals 1,8-di([5]trovacenyl)naphthalene (**6**), 1,5-di([5]trovacenyl)naphthalene (**7**), and 1,3-di([5]trovacenyl)benzene (**8**) and the monoradical 1-[5]trovacenylnaphthalene (**9**) have been prepared and studied by means of single-crystal X-ray diffraction (**6**, **8**, **9**), cyclic voltammetry, EPR spectroscopy, and magnetic susceptometry. Comparison of the magnetic properties of **6**−**9** reveals that π-stacking, as encountered in **6**, largely enhances exchange interaction between the two singly occupied V($3d_{z^2}$) orbitals. The effect of π-stacking on the electrochemical properties, as manifested in the redox splitting between consecutive electron transfer steps, is less pronounced. Redox splittings $\delta E_{1/2}$ for consecutive reductions exceed those for oxidations of binuclear trovacenes, $\delta E_{1/2}(2+/+, +/0)$ being apparent for π-stacked **6** only. Because of the orthogonality of the metal-centered redox orbitals V1(d_{z^2}) and V2(d_{z^2}) and the η^5-cyclopentadienyl π-orbitals, electro- and magnetocommunication are indirect processes. Electrocommunication rests on changes of the donor/acceptor properties of V1,V2 caused by oxidation or reduction which govern metal−ligand charge distribution; the latter changes are transmitted via the spacer. Magnetocommunication takes the form of antiferromagnetic coupling, which can be traced to spin polarization of filled π-orbitals of the bridge by orthogonal singly occupied vanadium $3d_{z^2}$ orbitals.

Introduction

Spectroscopic and electrochemical manifestations of π-stacking have been explored for organic as well as for organometallic molecules, the compounds **1**,[1−2] **2**,[3] and **3**,**4**[4] may serve as representative examples. Remarkably, $\pi-\pi$ interactions between stacked porphyrin rings and their metal complexes, which may lead to dimer formation, have aroused considerable interest because of their possible relation to enzyme function. The nature of $\pi-\pi$ interactions in general[5] and of dimeric cofacial porphyrins in particular[6] has been discussed extensively. An asset of binuclear metallocenes of type **3** is the possibility to use central-metal related spectroscopic techniques to gauge the extent of stacking interactions; the respective methods have recently been reviewed.[7]

Our own contributions to the study of intramolecular communication are based on the use of trovacene [(*tro*pylium)*va*nadium(*cyclop*e*nt*adi*e*nyl), (η^7-C_7H_7)V-(η^5-C_5H_5)] **5** as a probe.[1,8] Its suitability derives from the orbitally nondegenerate ground state $^2A_1$, the presence of the magnetic nucleus ^{51}V (I = 7/2) in high abundance (99.75%), the attendant favorable EPR properties, comparatively low sensitivity to air, and the ease of functionalization. Therefore, access to a large variety of di- and oligonuclear species featuring diverse spacers is envisaged. Here we report on the synthesis and characterization of two regioisomers in which [5]tro-

† Dedicated to Prof. G. Huttner on the occasion of his 65th birthday.

* To whom correspondence should be addressed. E-mail: eb@chemie.uni-marburg.de.

(1) Trovacene Chemistry. 4. Part 3: Elschenbroich, C.; Wolf, M.; Burghaus, O.; Harms, K.; Pebler, J. *Eur. J. Inorg. Chem.* **1999**, 2173.

(2) Gerson, F. *Topics Curr. Chem.* **1983**, *115*, 57.

(3) (a) Boekelheide, V. *Pure Appl. Chem.* **1986**, *58*, 1. (b) Voegeli, R. H.; Kang, H. C.; Finke, R. G.; Boekelheide, V. *J. Am. Chem. Soc.* **1986**, *108*, 7010. (c) Schröder, A.; Mekelburger, H.-B.; Vögtle, F. *Top. Curr. Chem.* **1994**, *172*, 41. (d) Kang, H. C.; Plitzko, K.-D.; Boekelheide, V.; Higuchi, H.; Misumi, S. *J. Organomet. Chem.* **1987**, *321*, 79.

(4) Lee, M.-T.; Foxman, B. M.; Rosenblum, M. *Organometallics* **1985**, *4*, 539. (b) Arnold, R.; Foxman, B. M.; Rosenblum, M.; Euler, W. B. *Organometallics* **1988**, *7*, 1253. (c) Herber, R. H.; Nowik, I.; Rosenblum, M. *Organometallics* **2002**, *21*, 846.

(5) (a) Misumi, S.; Otsubo, T. *Acc. Chem. Res.* **1978**, *11*, 251. (b) Heilbronner, E.; Yang, Z. *Top. Curr. Chem.* **1983**, *115*, 1. (c) Hunter, C. A.; Meah, M. N.; Sanders, J. K. M. *J. Am. Chem. Soc.* **1990**, *112*, 5773. (d) Cozzi, F.; Cinquini, M.; Annunziata, R.; Siegel, J. S. J. *Am. Chem. Soc.* **1993**, *115*, 5330. (e) Hunter, C. A. *Chem. Soc. Rev.* **1994**, *27*, 101. (f) Hunter, C. A. *J. Chem. Soc., Perkin Trans. 2* **2001**, 651. (g) Tsuzuki, S.; Honda, K.; Uchimaru, T.; Mikami, M.; Tanabe, K. *J. Am. Chem. Soc.* **2002**, *124*, 104.

(6) (a) Scheidt, W. R.; Geiger, D. K.; Lee, Y. L.; Reed, C. A.; Lang, G. *J. Am. Chem. Soc.* **1985**, *107*, 5693. (b) Gupta, G. P.; Lang, G.; Scheidt, R. W.; Geiger, D. K. *J. Chem. Phys.* **1985**, *83*, 5945. (c) Scheidt, W. R.; Lee, J. L. *Struct. Bonding* (*Berlin*) **1987**, *64*, 1. (d) Song, H.; Reed, C. A.; Scheidt, W. R. *J. Am. Chem. Soc.* **1989**, *111*, 6867. (e) Song, H.; Rath, N. P.; Reed, C. A.; Scheidt, W. R. *Inorg. Chem.* **1989**, *28*, 1839. (f) LeMest, Y.; L'Her, M.; Hendricks, N. H.; Kim, K.; Collman, J. P. *Inorg. Chem.* **1992**, *31*, 835. (g) Fletcher, J. T.; Therien, M. J. *Inorg. Chem.* **2002**, *41*, 331. (h) Gupta, G. P.; Lang, G.; Scheidt, W. R.; Geiger, D. K.; Reed, C. A. *J. Chem. Phys.* **1985**, *83*, 5945.

(7) Barlow, S.; O'Hare, D. *Chem. Rev.* **1997**, *97*, 637.

(8) (a) Elschenbroich, Ch.; Bilger, E.; Metz, B. *Organometallics* **1991**, *10*, 2823. (b) Elschenbroich, Ch.; Schiemann, O.; Burghaus, O.; Harms, K. *J. Am. Chem. Soc.* **1997**, *119*, 7452. (c) Elschenbroich, Ch.; Schiemann, O.; Burghaus, O.; Harms, K.; Pebler, J. *Organometallics* **1999**, *18*, 3273. (d) Elschenbroich, Ch.; Plackmeyer, J.; Harms, K.; Burghaus, O.; Pebler, J. *Organometallics*, submitted.

10.1021/om020520y CCC: $22.00
Publication on Web 11/20/2002

Scheme 1

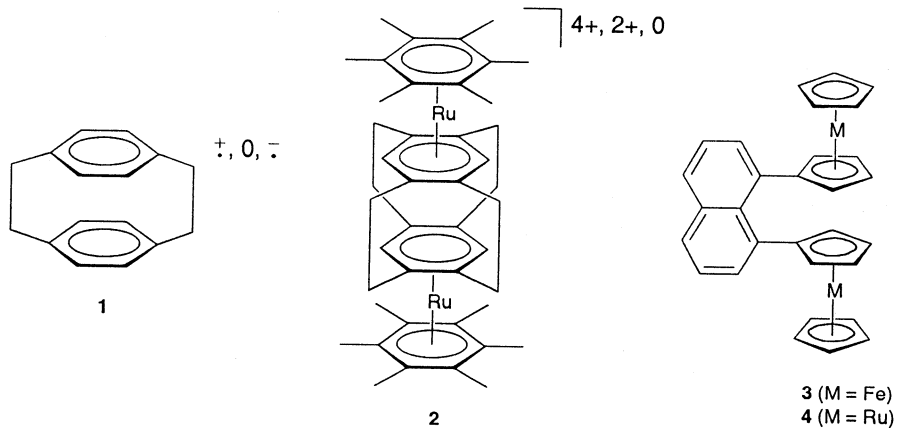

Scheme 2

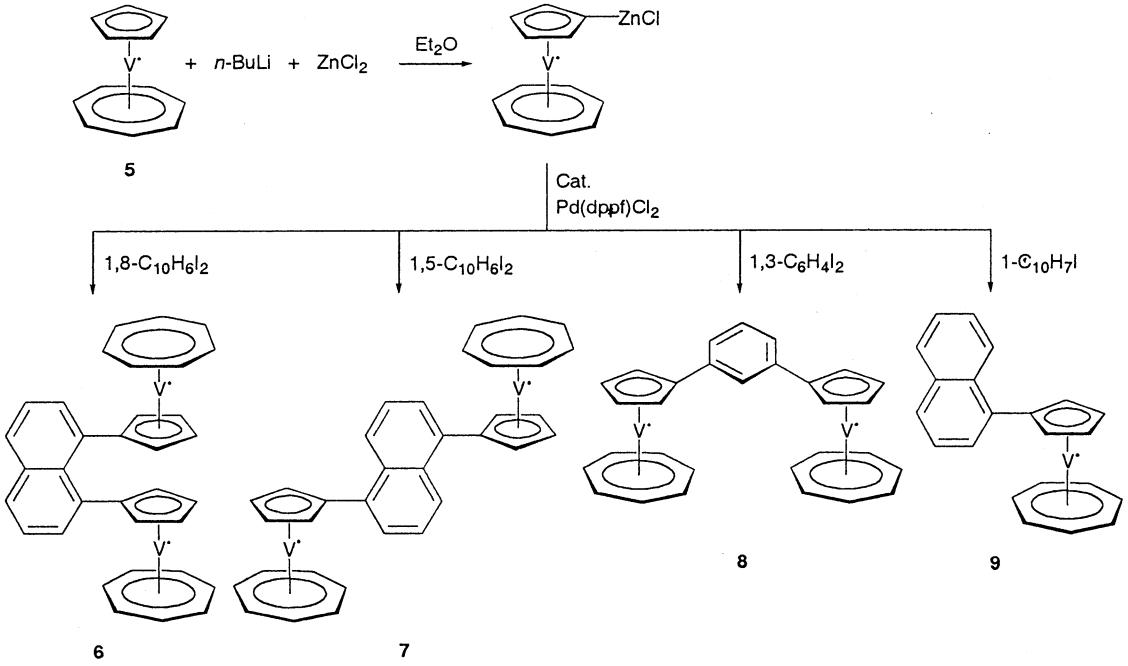

vacenyl units are linked to naphthalene in 1,8-(**6**) and 1,5-(**7**) positions, respectively. Whereas **6** is a biradical analogue of the stacked 1,8-dimetallocenylnaphthalenes **3** and **4**, π-stacking is absent in **7**. Obviously, a comparison of the electrochemical and magnetic properties of **6** and **7** should reveal to what extent face-to-face interactions between aromatic decks govern intramolecular communication. To this end, the measurement of exchange coupling J has been applied only rarely, inter-heme spin coupling in $\{[Fe(OEP)(2\text{-MeHIm})]^+\}_2$ dimers[6h] constituting an example (OEP = octaethylporphyrinate; 2-MeHIm = 2-methylimidazole).

Results and Discussion

The new trovacene derivatives **6**−**9** were prepared via the Negishi-Kumada route[9] (Scheme 2). Since the isomers **6** and **7** differ in the number of spacer atoms, we also synthesized 1,3-di([5]trovacenyl)benzene **8**,[10] which, like **6**, features a $(C, sp^2)_3$ unit linking the two trovacenyl cores. Alternatively, if the ipso-carbon atoms of the cyclopentadienyl rings are included in the count, the view may be taken that in **6** and **8** the two spin-bearing vanadium atoms are bridged by C_5 units. The mononuclear complex **9** was prepared as a reference molecule with the aim of eventually detecting leakage of spin density into the 1-naphthyl substituent. Furthermore, **9** constitutes the standard against which the redox potentials of the dinuclear complexes **6**−**8** should be assessed.

X-ray Crystallography. The solid-state structures of compounds **6**, **8**, and **9** are displayed in Figures 1−3; selected bond distances and angles are shown in the captions. The exceedingly low solubility of **7** in all common solvents prevented the growth of crystals suitable for a diffraction study. The dimensions of the trovacenyl groups in **6**, **8**, and **9** do not present noticeable differences from that of parent **5**. With regard to 1-[5]trovacenylnaphthalene **9** the only structural parameter worth mentioning is the dihedral angle $\Theta(C_5H_4/C_{10}H_7) = 79.3°$, which largely exceeds the corresponding

(9) Negishi, E. I. *Acc. Chem. Res.* **1982**, *15*, 340. Negishi, E. I. In *Organozinc Reagents. A Practical Approach*; Knochel, P., Jones, P., Eds.; Oxford University Press: Oxford, U.K., 1999; Chapter 11.

(10) The numbers in brackets indicate the site of substitution: [5]-trovacenyl is functionalized at the cyclopentadienyl and [7]trovacenyl at the cycloheptatrienyl ligand.

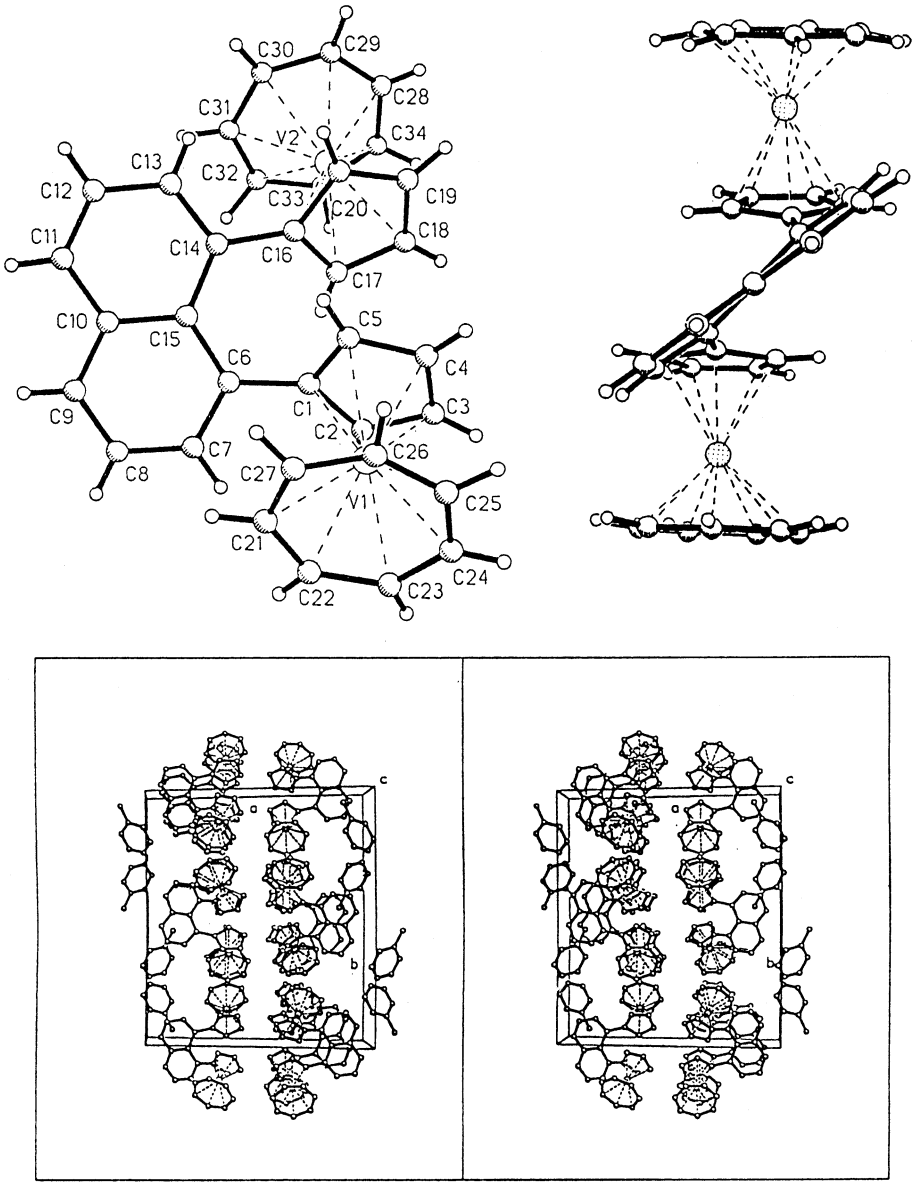

Figure 1. Molecular structure of 1,8-di([5]trovacenyl)naphthalene (**6**) in the crystal (SHAKAL drawings, numbering scheme, and stereoplot of the unit cell). Selected bond lengths (Å) and bond angles (deg): V1−C1 2.306(2); V1−C2 2.269(2); V1−C3 2.250(3); V1−C4 2.247(3); V1−C5 2.266(3); V1−C21 2.179(3); V1−C22 2.182(3); V1−C23 2.178(3); V1−C24 2.192(3); V1−C25 2.187(3); V1−C26 2.178(3); V1−C27 2.170(3); C−C(C_5, mean) 141.1(4); C−C(C_7, mean) 139.9(4); C1−C6 148.6(3); C_5(centroid)−V1 1.923(1); C_7(centroid)−V1 1.466(1); dimensions of trovacene 2 are identical within the error margin; intercentroid distance C_5(trovacene 1)···C_5(trovacene 2) 3.432; dihedral angles C_5(trovacene 1), naphthalene (best plane) 42.5; C_5(trovacene 2), naphthalene (best plane) 40.5.

angle $\Theta(C_5H_4/C_6H_5) = 24.2°$ in [5]trovacenylbenzene.[1] Not surprisingly, the structure of **6** largely resembles its congener **3**.[4a] It may be described as two stacked but laterally slipped trovacene units which are linked by a 1,8-naphthalenediyl lever. The twist angle between the cyclopentadienyl(Cp) and naphthalene(Naph) planes amounts to 40.5° compared with 42.5°; it is somewhat smaller than that in **3** (45.0° compared with 47.0°). Since the immediate environment at the Cp-Naph junction is identical for **3** and **6**, the small difference in the dihedral angles must be traced to packing effects. The mean interplanar distance of the η^5-Cp rings in **6** amounts to 343 pm, and repulsive interactions cause sizable puckering of the bridging naphthalene unit as well as deviations of the $C_{Naph}-C_{Cp}$ bond vectors from coplanarity with the naphthalene frame: the deviations of the Cp-ipso carbon atoms C1 and C16 from the best naphthalene plane amount to 0.54 and −0.53 Å, respectively. This translates into an angle of 31° between the vectors C1−C6 and C14−C16. Yet, whereas the trovacene units in **6** deviate markedly from an ideal face-to-face disposition, considerable stacking interaction nonetheless exists, which will be used in the sequel to rationalize the physical data.

1,3-Di([5]trovacenyl)benzene **8** in the solid state adopts a syn conformation approaching an ideal side-on disposition of the sandwich units (Figure 2). The bridging benzene and the two η^5-Cp rings deviate only marginally (7.4°) from coplanarity. The η^7-C_7H_7 rings in **8** display rotational disorder.

Redox Processes. All newly synthesized trovacene derivatives were subjected to cyclic voltammetry; elec-

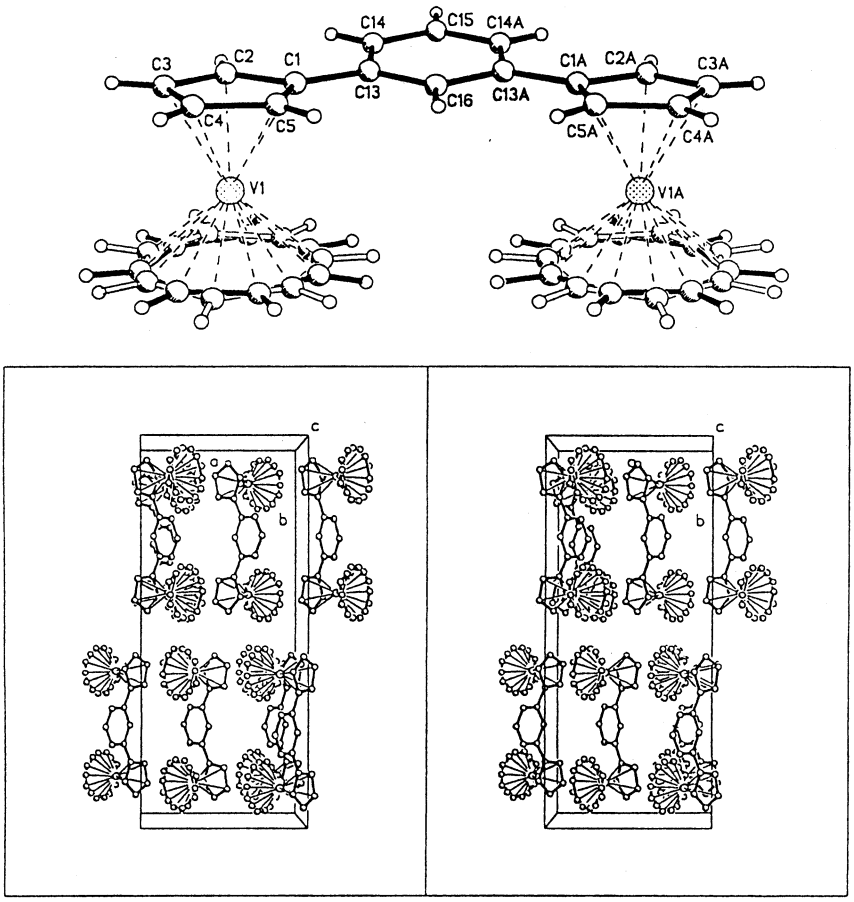

Figure 2. Molecular structure of 1,3-di([5]trovacenyl)benzene (**8**) in the crystal (SHAKAL drawing, numbering scheme, and stereoplot of the unit cell). Selected bond lengths (Å) and bond angles (deg): V1−C(C_5, mean) 2.256(4); V1−C(C_7, mean) 2.160(20); rotational disorder; C−C(C_5, mean) 1.413(2); C−C(C_7, mean) 1.407(20); C1−C13 1.479(5); C_5(centroid)−V1 1.9098(6); C_7(centroid)−V1 1.4402(6); dimensions of trovacene 1A are identical within the error margin. V1···V1A 7.2535-(11); dihedral angle C_5/C_6 7.4(2).

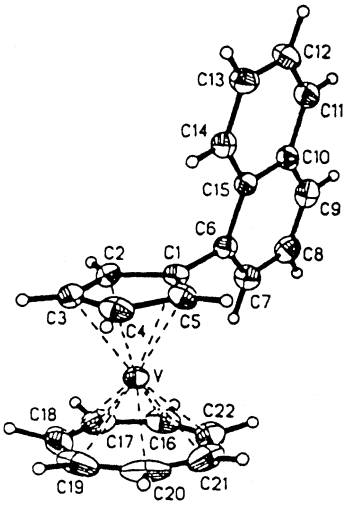

Figure 3. Molecular structure of 1-[5]trovacenylnaphthalene (**9**) in the crystal (SHAKAL drawing and numbering scheme). Selected bond lengths (Å) and bond angles (deg): V−C(C_5, mean) 226.5(3); V−C(C_7, mean) 218.5(3); C−C(C_5, mean) 142.0(4); C−C(C_7, mean) 140.6(6); C1−C6 148.7(4); dihedral angle C_5/naphthalene 79.3.

trochemical traces are depicted in Figure 4, and the corresponding data are found in Table 1. Due to consecutive redox processes of small potential differences, the degree of electrochemical reversibility and the number of electrons transferred cannot be assessed reliably. This derives from the fact that electrocommunication, which is clearly discernible for the directly linked [5−5]bitrovacene[8c] and its [7−7]isomer,[8d] is attenuated in the case of spacered bitrovacenes. Furthermore, the reduction potentials $E_{1/2}(0/-)$ are very similar for trovacene (−2.55 V) and for naphthalene (−2.48 V vs SCE). Secondary and tertiary reductions close to the cathodic limit of the medium also distort the shapes of the waves and complicate analyses. Therefore, only qualitative considerations will be offered.

Metal-centered primary *oxidations* of the complexes **7**, **8**, and **9** give rise to unresolved single waves. Only in the case of the stacked binuclear complex **6** is the presence of two overlapping waves discernible, differing by $\delta E_{1/2}(2+/+, +/0) \leq 70$ mV. Clearly, therefore, the head-on disposition of two trovacene units in **6** effects somewhat more extensive electrocommunication than the side-on arrangement in **7**. The gradation is surprisingly small, however. Although the one-electron oxidations for **6**−**9** all take place in a 50 mV bracket, a consistent interpretation of the individual values may be proposed. Accordingly, the anodic shift of the potential $E_{1/2}(+/0,$ **9**), relative to $E_{1/2}(+/0,$ **5**), may be traced to electron delocalization into the naphthyl substituent, whereby electron density in the trovacenyl unit is somewhat decreased. The same effect is operative in **7**. In **9** and **7**, rotation about the naphthyl−trovacene bond

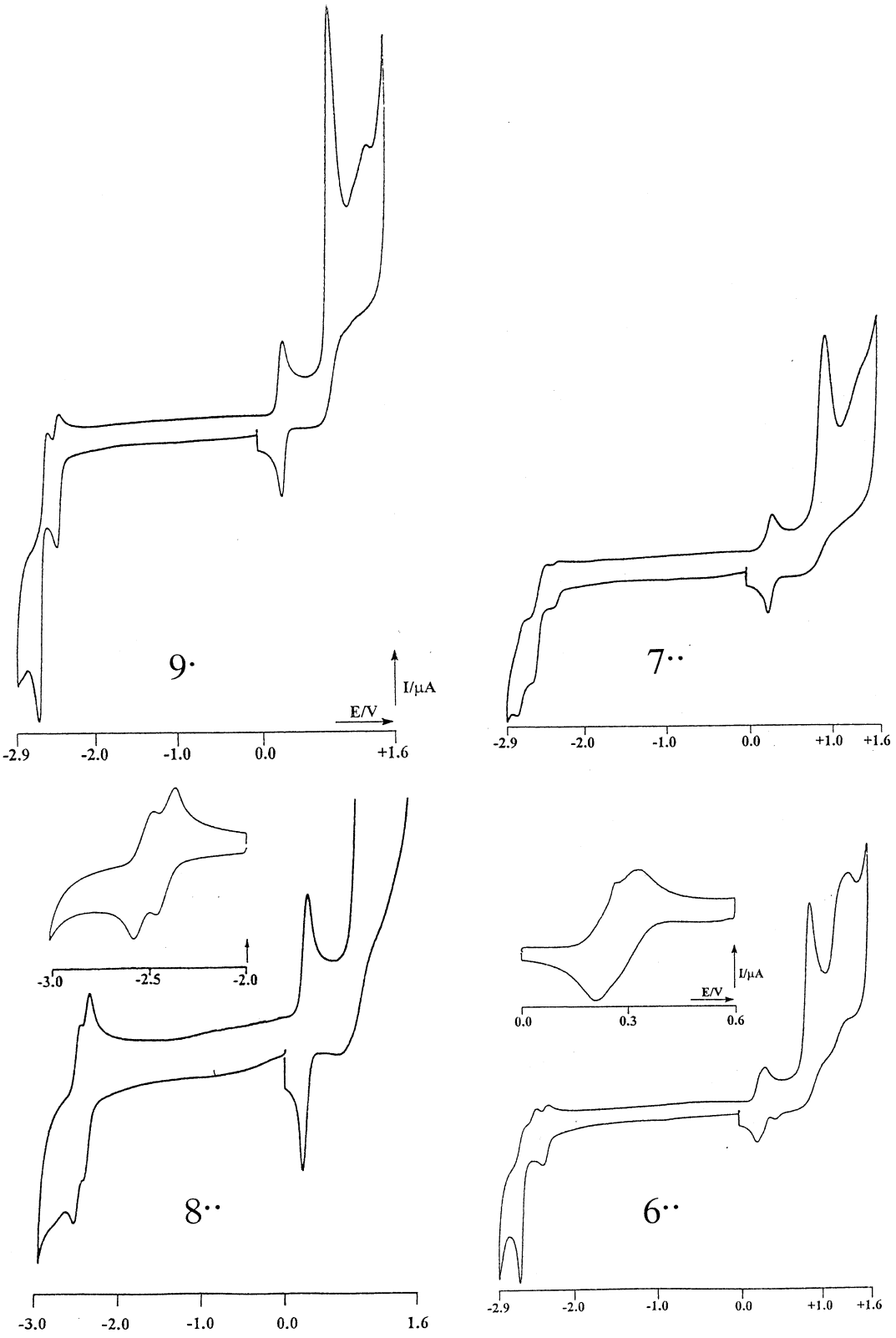

Figure 4. Cyclic voltammograms for 1-[5]trovacenylnaphthalene (**9**), 1,5-di([5]trovacenyl)naphthalene (**7**), 1,3-di([5]-trovacenyl)benzene (**8**), and 1,8-di([5]trovacenyl)naphthalene (**6**). For the electrochemical data see Table 1.

is only slightly hindered; therefore, conformations conducive to π-conjugation are feasible. Contrarily, for the π-stacked complex **6**, steric hindrance will prevent the trovacenyl units from adopting a conformation in which the cyclopentadienyl and naphthyl π-electron systems are coplanar. It may be argued that for **6** the twisted form found in the crystal is caused by packing forces and that, in fluid solution, a conformation in which the naphthyl and cyclopentadienyl rings are orthogonal will be favored. Transfer of π-electron density into the naphthyl unit is then hampered, and **5** and **6** are oxidized at almost identical potential. The argument put

Table 1. Cyclovoltammetric Data for Trovacene 5 and Its Derivatives 6−9[a]

	5	6	7	8	9
$E_{1/2}$(+/0)/V	0.26	0.24	0.31	0.27	0.31
ΔE_p/mV	64	57	68	71	76
r	1	≈0.9	0.9	1	1
$E_{1/2}$(2+/+)/V		0.30	0.31	0.27	
ΔE_p/mV		61	68	71	
r		≈0.9	0.9	1	
$E_{pa,1}$/V		1.0	0.99	1.0	1.0
$E_{pa,2}$/V		1.47	1.36		
$E_{1/2}$(0/−)/V	−2.55	−2.32	−2.30	−2.43	−2.35
ΔE_p/mV	66	66	64	63	57

[a] DME/(n-Bu)$_4$NClO$_4$, −40 °C, 100 mV/s, versus SCE. $r = i_a/i_c$ (ratio of peak currents). Additional peak potentials E_p (V) (reversibility criteria not applicable): **6**, $E_{pc} = -2.65$ (large peak current); $E_{pa} = -2.59$, −2.46. **7**, $E_{pc} = -2.60$ (large peak current), −2.78; $E_{pa} = -2.47$, −2.70. **8**, $E_{pc} = -2.59$; $E_{pa} = -2.48$. **9**, $E_{pc} = -2.68$ (large peak current); $E_{pa} = -2.53$.

forward to explain the anodic shift of $E_{1/2}$(+/0, **7**) also applies to **8**; due to the reduced electron-accepting capacity of benzene, compared to naphthalene, the cathodic shift of $E_{1/2}$(+/0, **8**) is only marginal, however.

An interpretation of the electrochemical data for *reductions* is impeded by the aforementioned problem in assigning the close lying waves to specific ET-steps (metal- or bridge-centered?). Reduction of the separate building blocks occurs at $E_{1/2}$(0/−, trovacene **5**) = −2.55 V and $E_{1/2}$(0/−, naphthalene) = −2.48 V. Consideration of the electron-donating nature of **5** and the electron-accepting property of naphthalene and of the anodic shift of $E_{1/2}$(−/0) for all derivatives containing both units suggests that the first reduction step is trovacene-centered. In the case of **9** the second wave must then be assigned to naphthalene reduction, the cathodic shift relative to free naphthalene being caused by the trovacene$^-$ substituent. Why the cathodic peak current seems to imply a 2e process here is not clear in view of the fact that **9** contains one naphthalene and one trovacene unit only. In the cathodic regime for **7**, three cathodic and three anodic peaks separated by ∼200 mV are barely resolved. Whereas the first reduction probably involves the vanadium atom, assignment of the second and third step is impractical. Very similar redox behavior is displayed by **6**, while the first reduction step for **8** exhibits a cathodic shift of 110 mV relative to **6** and **7**. Thus, for **6** and **7** two effects appear to cancel each other: **6** features a shorter intermetal distance and a π-stacking contact but impaired π-conjugation via the naphthalenediyl bridge because of near orthogonality. In **7**, on the other hand, the intermetal distance and the number of intervening sp^2-carbon atoms are larger, but ease of rotation about the C(trovacene)−C(naphthalene) bonds contributes conformations that are favorable to π-conjugation. In **8**, relative ease of conformational change and the presence of a short (C, sp^2)$_3$ unit separating the trovacenes are combined with the effect that the reduction of the first trovacene moiety is rendered somewhat more difficult by the presence of the second electron-releasing trovacene.

It remains to emphasize that the redox properties of spacered diferrocenes[4a,12] and of ditrovacenes cannot be compared directly because of differing frontier orbital characteristics. Whereas trovacene ($e_2^4a_1^1$) possesses a SOMO V($3d_{z^2}$) practically devoid of metal−ligand mixing and therefore may undergo metal-centered oxidation *and* reduction, ferrocene ($e_{2g}^4a_{1g}^2$) upon oxidation yields the configuration $e_{2g}^3a_{1g}^2$ with considerable metal−ligand mixing of the redox orbital, which explains the larger redox splitting in the oxidation of **3**. Furthermore, the 18 VE configuration of ferrocenes is not prone to reduction, at least not within the "normal" electrochemical window (cathodic limit ≈ −3.0 V).

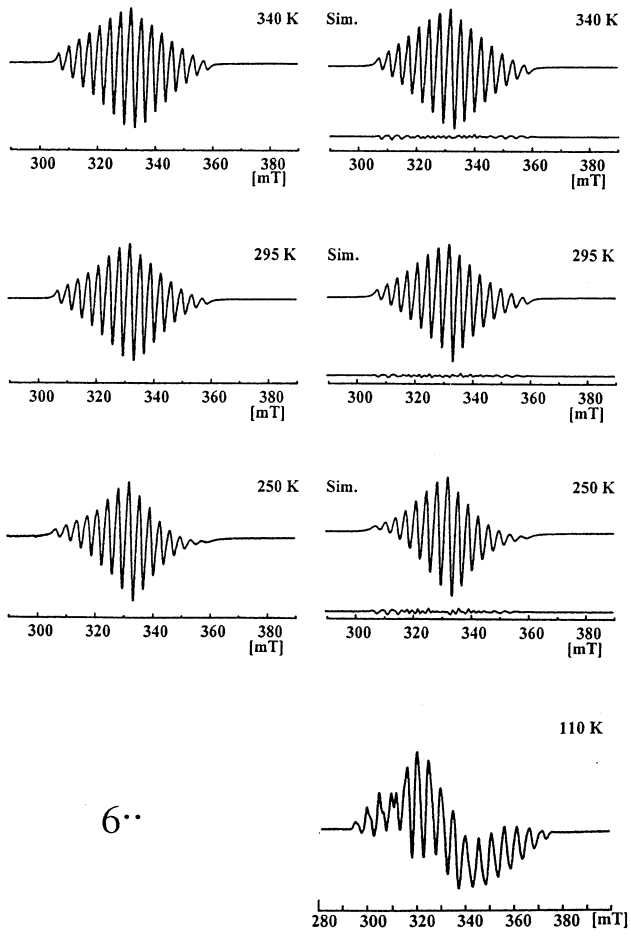

Figure 5. EPR spectra of 1,8-di([5]trovacenyl)naphthalene (**6**) in fluid and rigid solution (toluene) and their simulated traces; parameters are collected in Table 2.

At this point one may ask how electrocommunication between the two sites actually arises, in view of the fact that the redox orbitals are metal-centered and nearly orthogonal to the cyclopentadienyl π-electron systems which form the links between the metals and the spacer. Conceivably, changes in the occupation of the redox orbitals V1(d_{z^2}) and V2(d_{z^2}) and the attendant change in local charge modify the donor/acceptor characteristics of the central metals and therefore influence the metal−ligand charge distribution, in this way providing a way by which redox processes at V1 may modulate redox processes at V2. This is an indirect mechanism, however, and therefore redox splittings are expected to be small. This contrasts with the considerably larger redox splittings that are encountered when the metal redox orbitals possess correct symmetry for d(π)−p(π) overlap with the bridging ligand.[11]

(11) McCleverty, J. A.; Ward, M. D. *Acc. Chem. Res.* **1998**, *31*, 842. Campagna, S.; Giuffrida, G. *Coord. Chem. Rev.* **1994**, *136*, 517.
(12) Patoux, C.; Coudret, C.; Launay, J.-P.; Joachim, C.; Gourdon, A. *Inorg. Chem.* **1997**, *36*, 5037.

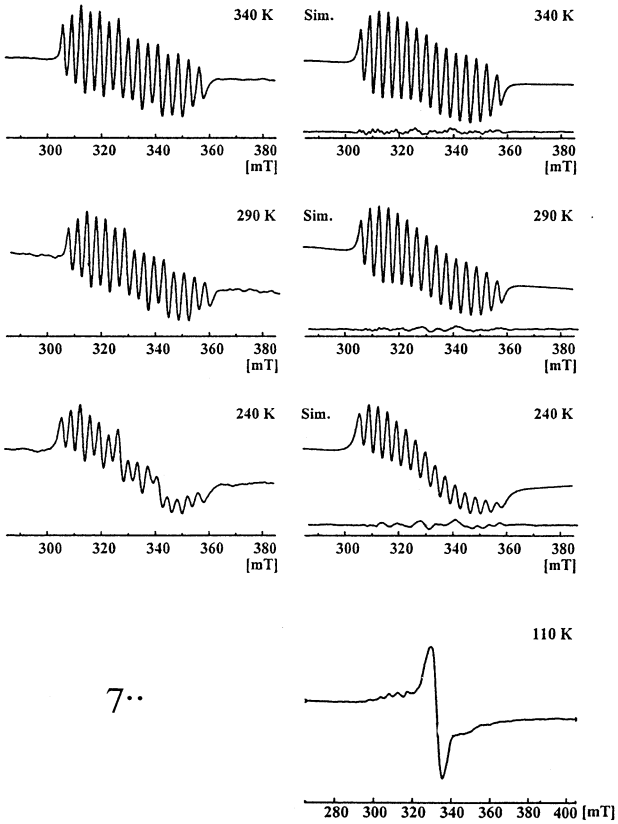

Figure 6. EPR spectra of 1,5-di([5]trovacenyl)naphthalene (**7**) in fluid and rigid solution (toluene) and their simulated traces; parameters are collected in Table 2.

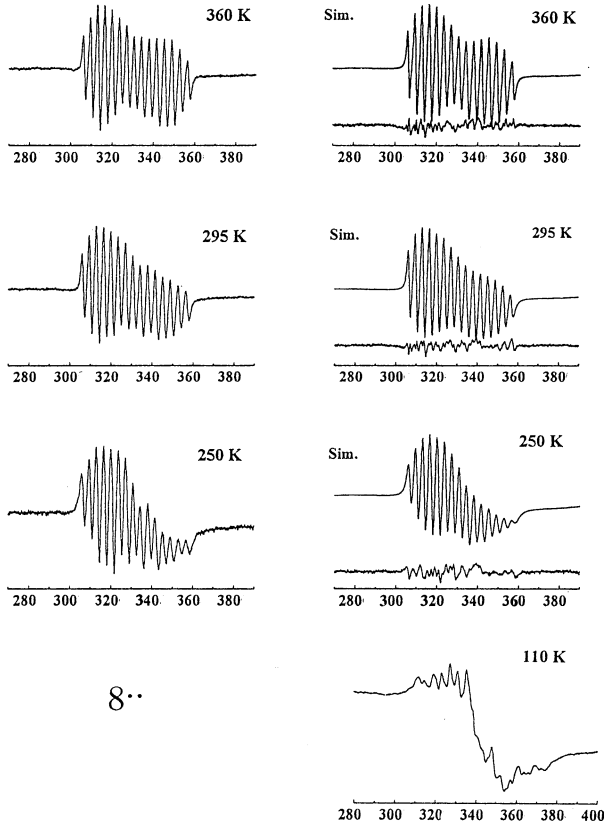

Figure 7. EPR spectra of 1,3-di([5]trovacenyl)naphthalene (**8**) in fluid and rigid solution (toluene) and their simulated traces; parameters are collected in Table 2.

EPR Spectra and Magnetic Susceptibility. Exchange interactions can be studied on a molecular level by EPR and in the bulk by magnetic susceptometry. Apart from the vastly higher sensitivity of the former, the two methods differ in that EPR describes the magnetic properties of individual molecules, eventually reflecting their conformational freedom in the absence of intermolecular interactions, whereas magnetic susceptibility deals with the conformation dictated by packing forces and may also have to consider intermolecular magnetic exchange.

Temperature-dependent EPR spectra of **6**−**8** in fluid solution and their simulations are shown in Figures 5−7, and the EPR parameters are collected in Table 2. The coefficients $a-d$ of the line width equation

$$\Delta B = a + b[m_I(1) + m_I(2)] + c[m_I(1) + m_I(2)]^2 + d[m_I(1) - m_I(2)]^2$$

are also given. This relation treats the dependence of the line widths on the anisotropies of the g-tensor and the hyperfine interaction (a, b, c), and its consideration is indispensable for a satisfactory fit of the experimental spectra. Fluctuations of the exchange interaction J may give rise to alternating line widths. This effect is handled by inclusion of the parameter d.[13]

Plots of χ^{-1} versus temperature for **6**−**8** and the fits of the Bleaney−Bowers equation

$$\chi = \frac{2N_A\mu_B{}^2g^2 3\exp(2J/kT)}{3kT[1 + 3\exp(2J/kT)]} \cdot \frac{T}{(T - \Theta)}$$

Table 2. EPR Data for Trovacene 5 and the Derivatives 6−9[a]

	T/K	$\langle g \rangle$	$a(^{51}V)$/mT	$\lvert J \rvert$/cm^{-1}	b	c	d
5•	295	1.987	−6.98				
9•	295	1.980	−7.22				
6••	250	1.9784	−7.17	2.15	−0.580	0.298	−0.285
	295	1.9789	−7.17	2.22	−0.415	0.060	−0.272
	330	1.9788	−7.18	2.16	−0.301	0.0056	−0.202
7••	240	1.9800	−7.23	0.72	−1.685	0.029	1.89
	290	1.9782	−7.22	0.63	−0.608	0.056	1.31
	30	1.9805	−7.22	0.44	−0.413	−0.08	1.07
8••	250	1.982	−7.20	0.61	−1.99	0.12	0.70
	295	1.982	−7.20	0.48	−0.82	−0.11	0.55
	360	1.982	−7.20	0.35	−0.37	−0.14	0.24

[a] Solvent: toluene. a, b, and c are the coefficients in the line width equation which, in the spectral simulations, allow for $m_\pm$-dependence of the line widths.

are reproduced in Figure 8, and the parameters are given in the captions. The interaction is antiferromagnetic in all cases; exchange coupling, as extracted from the EPR spectra recorded in fluid solution at ambient temperature, follows the gradation

$$J(\mathbf{6}, |2.22|) > J(\mathbf{7}, |0.63|) \approx J(\mathbf{8}, |0.48|)\ [\text{cm}^{-1}]$$

Compound **6** stands out in possessing a π-stacked structure to which the comparatively large value of J therefore must be attributed. The interpretation is

(13) Mabbs, F. E. *Chem. Soc. Rev.* **1993**, *22*, 313.

Table 3. Crystallographic Data for Compounds $6^{\bullet\bullet}\cdot C_7H_8$, $8^{\bullet\bullet}$, and $9^{\bullet}$

	$6^{\bullet\bullet}\cdot C_7H_8$	$8^{\bullet\bullet}$	$9^{\bullet}$
habitus, color	thin plate, red-green	thin plate, dark	nugget, violet
cryst size [mm^3]	0.16 × 0.15 × 0.07	0.50 × 0.30 × 0.03	0.21 × 0.15 × 0.09
cryst syst	monoclinic	orthorhombic	orthorhombic
space group	$P2_1/c$, $Z = 4$	$Pnma$, $Z = 8$	$Fdd2$, $Z = 16$
unit cell [Å, deg]	$a = 18.2179(17)$	$a = 10.5710(10)$	$a = 13.5510(10)$
	$b = 20.6897(12)$	$b = 24.873(3)$	$b = 67.397(6)$
	$c = 8.3505(8)$	$c = 8.5640(10)$	$c = 6.9222(6)$
	$\beta = 103.040(11)$		
volume	3066.3(4) Å^3	2251.8(4) Å^3	6322.0(9) Å^3
cell determination	5000 reflns	25 reflns	5000 reflns
empirical formula	$C_{41}H_{36}V_2$	$C_{30}H_{26}V_2$	$C_{22}H_{18}V$
fw	630.58	488.39	333.30
density(calcd) [Mg/m^3]	1.366	1.441	1.401
abs coeff [mm^{-1}]	0.638	0.846	0.624
$F(000)$	1312	1008	2768
θ range [deg]	2.28 to 25.92	2.52 to 25.00	2.42 to 26.00
index ranges	−22/22, −25/23, −10/10	0/12, −29/0, 0/10	−16/16, −82/82, −8/8
no. of collected reflns	21 855	2031	9397
no. of ind reflns [R(int)]	5922 [0.0604]	2030 [0.0006]	3090 [0.0460]
completeness [%]	99.1	89.0	99.7
observed reflns [$I > 2\sigma(I)$]	3480	1258	2625
no. of reflns for refinement	5922	2030	3090
abs corr	analytical		
T_{max} and T_{min}	0.9458 and 0.8977		
largest diff peak and hole [e Å^{-3}]	0.293 and −0.215	0.306 and −0.362	0.280 and −0.304
treatment of hydrogen atoms	located, isotropic refinement	calculated positions, fixed isotropic U's	located, isotropic refinement
no. of params	532	210	280
Flack param (abs struct)			0.00(3)
wR2 (all data)	wR2 = 0.0651	wR2 = 0.1132	wR2 = 0.0807
R1 [$I > 2\sigma(I)$]	R1 = 0.0340	R1 = 0.0470	R1 = 0.0330

based on the premise that the singly occupied a_1 orbital in trovacene **5** is a function of almost exclusive V($3d_{z^2}$) character.[14] This is because the basis orbitals of the benzene π set lie in the nodal region of the V(d_{z^2}) orbital, and metal−ligand orbital overlap therefore vanishes. Direct interaction between the two V(d_{z^2}) orbitals in binuclear **6** can also be neglected because of the large metal−metal distance of almost 700 pm. Therefore, an indirect coupling path must be devised. A mechanism that comes to mind is sketched in Figure 9.

Nonconjugated π-sytems which are forced into close proximity are encountered in the cyclophanes such as the prototypical **1**; transannular through-space $\pi-\pi$ interactions will result in the generation of bonding and antibonding sets.[15] Covalent interactions between stacked π-systems manifest themselves in the EPR spectra of cyclophane radical ions, which point at delocalization of the unpaired electron over both arene moieties.[16,17] This type of communication is inoperative in the V(d_{z^2})-(Cp(π)/Cp(π) V(d_{z^2}) unit, though, since for symmetry reasons spin transfer into the stacked π-ligands is vanishingly small. Rather, spin polarization of filled π-orbitals generated in the stacking interaction between the Cp rings, effected by the singly occupied V(d_{z^2}) orbitals, can lead to antiferromagnetic coupling.[18] In Figure 9 only the linear combination formed from the a_{2u} $C_5H_5^-$ π MOs is shown; the MOs from interactions between e_{1g} orbitals of $C_5H_5^-$ will be spin polarized as well, thereby generating an additional coupling path. The coupling mechanism proposed for **6** gains plausibility from a comparison with the binuclear complex **8**. In both **6** and **8**, the trovacenyl units are separated by a (C sp^2)$_3$ chain; they differ in the accessible conformations, however. Whereas for **6** only π-stacked forms are attainable, in **8** rotation about the C(trovacene)−C(arene) bonds is sterically hindered only to a small extent, enabling a syn conformation with side-on disposed trovacenes and coplanarity of the η^5-cyclopentadienyl and the bridging *m*-phenylene units to be realized. Nevertheless, J(**8**), derived from EPR in fluid solution, falls short of J(**6**) to a considerable extent. For the reason given for **6** (orthogonality of V(d_{z^2}) and the ligand π-orbitals), antiferromagnetic coupling in **8** may equally be traced to spin polarization of filled ligand π-orbitals. This effect is less pronounced for **8**, however, since it is transmitted via the bottleneck of the C(trovacene)−C(arene) bond, whereas in **6**, due to the face-to-face orientation of the η^5-cyclopentadienyl rings, all carbon p_π-orbitals contribute.

(14) (a) Rettig, M. F.; Stout, C. D.; Klug, A.; Farnham, P. *J. Am. Chem. Soc.* **1970**, *92*, 5100. The M(d_{z^2}) character of the a_{1g} frontier orbital for sandwich complexes in general is born out by numerous experimental studies as well as by quantum chemical calculations: (b) Muetterties, E. L.; Bleeke, J. R.; Wucherer, E. J.; Albright, T. A. *Chem. Rev.* **1982**, *82*, 499. (c) Cloke, F. G. N.; Dix, A. N.; Green, J. C.; Perutz, R. N.; Seddon, E. A. *Organometallics* **1983**, *2*, 1150. Green, M. L. H.; Ng, D. K. P. *Chem. Rev.* **1995**, *95*, 439. (d) Andrews, M. P.; Mattar, S. M.; Ozin, G. A. *J. Phys. Chem.* **1986**, *90*, 1037. (e) Pandey, R.; Rao, B. K.; Jena, P.; Blanco, A. M. *J. Am. Chem. Soc.* **2001**, *123*, 3799. (f) Lein, M.; Frunzke, J.; Trimoshkin, A.; Frenking, G. *Chem. Eur. J.* **2001**, *7*, 4155.

(15) Gleiter, R.; Schäfer, W. *Acc. Chem. Res.* **1990**, *23*, 369. Gleiter, R.; Kratz, D. *Acc. Chem. Res.* **1993**, *26*, 311.

(16) Gerson, F.; Martin, W. B., Jr. *J. Am. Chem. Soc.* **1969**, *91*, 1883. Gerson, F. *Top. Curr. Chem.* **1983**, *115*, 57.

(17) Interestingly, electron absorption and EPR spectroscopy has revealed the formation of the dimer radical cations (benzene)$_2^{\bullet+}$ and (naphthalene)$_2^{\bullet+}$, attesting to bonding interaction between stacked π-perimeters: Badger, B.; Brocklehurst, B. *Trans. Faraday Soc.* **1970**, *66*, 2939. Lewis, I. C.; Singer, L. S. *J. Chem. Phys.* **1965**, *43*, 2712.

(18) Supportive evidence for polarization of the filled MO e_{2g} by the singly occupied orbital a_{1g} in a (arene)$_2$M(d^5) unit is provided by a comparison of the sign and magnitudes of the hyperfine coupling constants a(^{1}H, CH_2) in [bis(cyclobuta-η^6-benzene)chromium]$^{\bullet+}$ and [(η^{12}-[2.2]paracyclophane)chromium]$^{\bullet+}$ and an interpretation in terms of conformation-dependent and conformation-independent contributions: Elschenbroich, Ch.; Koch, J.; Schneider, J.; Spangenberg, B.; Schiess, P. *J. Organomet. Chem.* **1986**, *317*, 41.

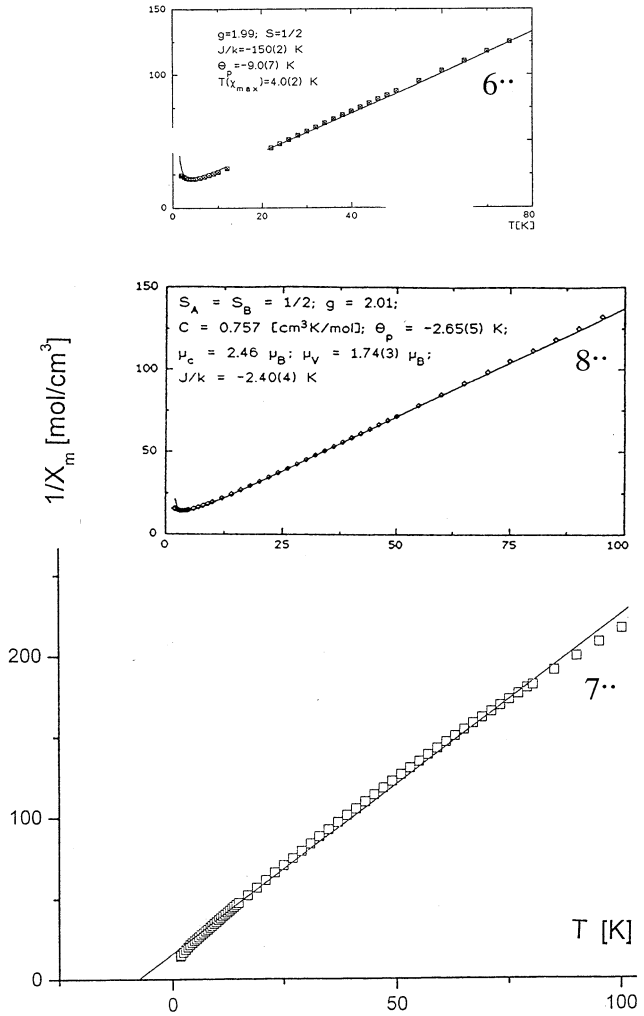

Figure 8. Temperature dependence of the inverse magnetic susceptibility χ^{-1} for **6**, **7**, and **8**. For parameters and fitting procedures see text.

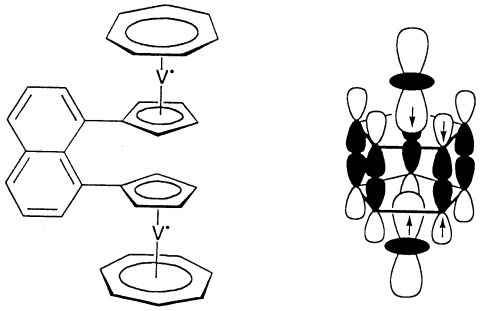

Figure 9. Antiferromagnetic coupling between two singly occupied V($3d_{z^2}$) orbitals, mediated by a π-stacked pair of cylopentadienyl rings with vanishing V($3d_{z^2}$)/Cp(a_{2u}) overlap as proposed for 1,8-di([5]trovacenyl)naphthalene (**6**).

Somewhat disturbingly, the gradation of *J*-values is reversed if, instead of EPR spectroscopy, the data from magnetic susceptometry are considered: $J_\chi(\mathbf{6}) = -1.04$, $J_\chi(\mathbf{8}) = -1.66\ cm^{-1}$. Note, however, that the results refer to differing states of aggregation. **6** in the solid experiences considerable slippage with attendant decrease of π-stacking interaction, whereas **8** forms a structure for which π-conjugation is maximal. This conformation, in which the two cyclopentadienyl and the *meta*-phenylene rings are coplanar, is tolerated by the small C−H compression strain inherent in this connectivity. It remains to comment on the low values of *J* for **7**. For this positional isomer of **6**, *J* obtained from EPR is small and in susceptometry too small to be determined. In the spirit of the aforesaid, this is plausible because in **7** π-stacking of the trovacenyl units is impossible for geometric reasons and conformations in which the η^5-cyclopentadienyl and the naphthalene π-systems are coplanar would suffer from severe strain caused by compression of the cyclopentadienyl$(C-H)_{ortho}$ and the naphthalene$(C-H)_{peri}$ bonds.

Interestingly, conformational preferences also seem to govern the temperature dependence of the fluid solution EPR spectra of **6**−**8**. Whereas for the fairly rigid complex **6**, temperature dependence is insignificant, **7** and **8** exhibit an increase in *J* by 63% and 74%, respectively, upon lowering the temperature by 100 °C. This points at the population, at lower temperatures, of conformations with smaller twist angles Θ and increased π-overlap, the limit of $\Theta = 0$ being reached by **8** in the crystal. Since J_χ(**7**) was found to be very small, it is tempting to predict that **7** in the crystal will assume a highly twisted structure.

By way of conclusion it may be stated that the influence the mutual disposition of two paramagnetic trovacene units—head-on (**6**) or side-on (**8**)—exerts on the degree of interaction depends on the physical mechanism of interaction. Whereas π-stacking, as encountered in **6**, boosts exchange coupling *J* to a considerable extent relative to nonstacked **8**, redox-splittings for **6** and **8** differ only marginally. Thus, magnetocommunication responds more sensitively to structural changes here than electrocommunication.

Experimental Section

Chemical manipulations and physical measurements were carried out using techniques and instruments specified previously.[1] Trovacene **5** was prepared from $(C_5H_5)V(CO)_4$[19a] according to the procedure given in the literature.[19b] 1,5-Diiodonaphthalene,[20] 1,8-diiodonaphthalene,[20] and the catalyst $Pd(dppf)Cl_2$[21] were also obtained as described previously (dppf = 1,1′-bis(diphenylphosphino)ferrocene). Anhydrous $ZnCl_2$ was generated by degassing molten $ZnCl_2 \cdot 4H_2O$ in vacuo. Cyclic voltammetry was performed under Ar protection in dimethoxyethane as a solvent, $(n\text{-}Bu)_4NClO_4$ serving as supporting electrolyte. A glassy carbon working electrode, a Pt counter electrode, and SCE reference electrode were employed. $E_{1/2}(Cp_2Fe^{+/0}) = 0.49$ vs SCE under these conditions.

1,8-Di([5]trovacenyl)naphthalene (6"). To a solution of trovacene (**5**; 435 mg, 2.1 mmol) in 130 mL of diethyl ether was added at room temperature 2.1 mL of a solution (1.55 M) of *n*-butyllithium in hexane. After stirring the mixture for 14 h, 3.7 mL of a solution (0.9 M) of anhydrous $ZnCl_2$ in tetrahydrofuran was added. Transmetalation was effected during 30 min, and 1,8-diiodonaphthalene (198 mg, 0.51 mmol) and $Pd(dppf)Cl_2$ (74 mg, 0.1 mol) in THF were added. The mixture was stirred at room temperature for 6 h and finally refluxed for 30 min. After removing the solvent in vacuo, the product was dissolved in toluene and chromatographed over Al_2O_3 (0% H_2O, column 2 × 15 cm). Unreacted trovacene was followed by a green zone, from which **6** was obtained. Yield:

(19) (a) Floriani, C.; Mange, V. *Inorg. Synth.* **1991**, *28*, 263. Floriani, C. *J. Chem. Soc., Dalton Trans.* **1976**, 1046. (b) King, R. B.; Stone, F. G. A. *J. Am. Chem. Soc.* **1959**, *81*, 5263.

(20) House, H.; Koepsell, D. G.; Campbell, W. J. *J. Org. Chem.* **1972**, *37*, 1003.

(21) Hayashi, T.; Konishi, M.; Kumada, M. *Tetrahedron Lett.* **1979**, *21*, 1871.

175 mg (0.33 mmol, 31%) of red-green dichroic crystals. MS (EI, 70 eV): *m*/*z* (relative intensity) 538 (M^+, 87.3), 447 ($M^+ - C_7H_7$, 100), 269 (M^{2+}, 23), 142 ($C_7H_7V^+$, 54.7). MS (high resolution] calcd 538.10703, found 538.10747 (^{12}C). IR (KBr): 3081, 3044(w), 1760−1580(w) 1500−1310(w), 1261, 1091, 1054, 1031, 1015(m), 823, 802, 779, 762(m), 488, 451, 432, 418(w). Anal. Calcd for $C_{34}H_{28}V_2$ (538.48): C, 75.84; H, 5.24. Found: C, 75.21; H, 5.13. For EPR and CV see text.

1,5-Di([5]trovacenyl)naphthalene (7••). By a procedure identical to that given for **6**, except for the use of 1,5-diiodonaphthalene instead of the 1,8-isomer, **7** was obtained in 16% yield as a green, microcrystalline product. MS (EI, 70 eV): *m*/*z* (relative intensity) 538 (M^+, 100), 269 (M^{2+}, 23.2). Anal. Calcd for $C_{34}H_{28}V_2$ (538.48): C, 75.84, H, 5.24. Found: C, 74.91; H, 5.72.

1-[5]Trovacenylnaphthalene (9•). The preparation of **9** followed the instructions given for **6**. From trovacene (280 mg, 1.35 mmol), *n*-butyllithium (1.4 mL of a 1.55 M solution in hexane), $ZnCl_2$ (0.8 mL of a 0.9 M solution in THF), 1-iodonaphthalene (170 mg, 0.67 mmol), and Pd(dppf)Cl_2 (51 mg, 0.07 mmol) a product mixture was obtained, which was separated by column chromatography (Al_2O_3, 0% H_2O, 2 × 25 cm). Elution by means of 1:1 toluene/petroleum ether delivered **9** in the second zone. Layering a solution of **9** in toluene with *n*-pentane produced red-green dichroic cubes. Yield: 189 mg (0.57 mmol, 42%). MS (EI, 70 eV): *m*/*z* (relative intensity) 333 (M^+, 100), 166 (M^{2+}, 3.4), 51 (V^+, 14). MS (high resolution): calcd 333.08436, found 333.08363 (^{12}C). IR (KBr): 3101, 3089-(w), 2956(m), 1765−1600(w), 1591(w), 1393(m), 1052(s), 796, 788, 774(s), 470, 439, 419(w). Anal. Calcd for $C_{22}H_{18}V$ (333.33): C, 79.27; H 5.44. Found: C, 78.18; H 5.80.

1,3-Di([5]trovacenyl)benzene (8••). Trovacene (300 mg, 1.4 mol) in 50 mL of diethyl ether was lithiated during 10 h at room temperature by 0.9 mL of a solution of *n*-butyllithium (1.6 M) in hexane. Transmetalation was effected by addition of 1.6 mL of a solution (0.9 M) of anhydrous $ZnCl_2$ in THF. To the resulting mixture was added a solution of 1,3-diiodobenzene (115 mg, 0.35 mmol) and Pd(dppf)Cl_2 (10 mg, 0.013 mmol) in 20 mL of THF. After refluxing for 1 h, the solvent was removed in vacuo and the residue taken up in 5 mL of toluene. Chromatography over Al_2O_3 (0% H_2O, column 2.5 × 30 cm) effected the separation of unreacted **5** (first zone, elution by benzene) from the product **8** (second zone, elution by benzene/THF, 15:1). Recrystallization from THF at 0 °C afforded **8** as violet platelets. Yield: 158 mg (0.32 mmol, 40%). MS (EI, 70 eV): *m*/*z* (relative intensity) 488 (M^+, 100), 244 (M^{2+}, 15), 51 (V^+, 10). IR (KBr): 3041(w), 1700−1638(w), 1602(m), 782(s), 491(w), 468(w), 442(m), 424(m). Anal. Calcd for $C_{30}H_{26}V_2$ (488.42): C, 73.77; H, 5.37. Found: C, 73.65; H, 5.29.

X-ray Crystallographic Study of 6••·C_7H_8, 8••, and 9•. Data were collected at 193 K on a STOE IPDS or ENRAF NONIUS CAD4 (**8••**) diffractometer using Mo Kα radiation. The structures were solved using direct methods and refined on F^2 values using the full matrix least-squares method. For compound **8••** a 2-fold disorder of the seven-membered rings has been refined.

Programs used: SHELXS-97 and SHELXL-97 (G. M. Sheldrick, University of Göttingen, Germany, 1997), STOE IPDS software (STOE & CIE GmbH, Darmstadt, Germany, 1999), CAD4 EXPRESS (Enraf Nonius, Delft, The Netherlands, 1994), SHELXTL 5.02 (Siemens Analytical X-ray Instruments Inc., Madison, WI, 1996).

Acknowledgment. This work has been supported by the Volkswagen Foundation and the Fonds der Chemischen Industrie.

Supporting Information Available: Tables giving crystal data and details of the structure determinations, positional and thermal parameters, and all bond distances and angles for **6**, **8**, and **9**. This material is available free of charge via the Internet at http://pubs.acs.org.

OM020520Y